Centrifugal Micromixer

By *Stefan Haeberle**, *Thilo Brenner*, *Hans-Peter Schlosser*, *Roland Zengerle*, and *Jens Ducrée*

We present a modular centrifugal micromixer comprising a mixing unit hosting a planar network of low-aspect-ratio microfluidic channels ("disk"), a fixed rotating drive ("player") and contact-free dispensers for the continuous feed of educts. The modular setup allows a simple fabrication and a child's play exchange of the mixing unit. High-speed micromixing is powered by the Coriolis force at volume throughputs of up to milliliters per minute and microchannel! These outstanding characteristics are demonstrated by experiments and accompanying CFD-simulations.

1 Introduction

The often cited incentives for running reactions in a miniaturized format are the deliberate exploitation of microfluidic phenomena as well as the tight control of mass and heat transfer, allowing to run chemical reactions under more intense ("aggressive") conditions. Such a process intensification bears a clear potential to improve the selectivity and the conversion rates as well as the purity of reaction products. In addition, entirely new reaction pathways may be pursued. In prospect of these unique technological opportunities, the interdisciplinary and diverse field of chemical micro process engineering has attracted appreciable academic and commercial interest [1–7].

The principle underlying the majority of concepts for volume synthesis is the multi-lamination of pressure-driven continuous flows into a vector of alternating thin lamellae [8–13]. These lamellae are usually shaped by the flow through 3-dimensional architectures of narrow guide structures displaying high aspect ratios to maximize throughput. However, the low absolute volume throughput still remains one major drawback of microreaction technology, which proves to be hard to compensate by numbering-up strategies for technical as well as economical reasons.

In this work, we introduce a novel, active mixing concept in planar networks of simple, low-aspect-ratio guide channels exhibiting comparatively large cross sections. This continuous flow scheme uses the centrifugal volume force generated by the rotating drive to both, pump and mix the liquid educts [14–18]. The merely hydrodynamically induced mixing roots in the velocity-dependent Coriolis pseudo force impacting flows in the rotating frame of reference [19, 20]. Due to the high flow rates attributed to the favorable interplay of the strong centrifugal force with the large channel cross section, our experiments and accompanying simulations demonstrate high throughputs at extremely reduced mixing times.

The fabrication of the setup is greatly facilitated by the modular concept, assigning the active components to a reusable macroscopic drive unit resembling a conventional centrifuge while the micromachining can focus on its genuine strength, the accurate replication of passive, "2.5-dimensional" and low-aspect-ratio microstructures. The rugged modular concept without pressure-tight interfaces also facilitates the quick exchange of the mixing units, thus minimizing down-times.

The paper begins with an outline of the centrifugal pumping principle and the intrinsic action of the Coriolis pseudo force (Sect. 2). Next, the experimental setup and the flow scheme implementing the Coriolis-based mixing is illustrated (Sect. 3) and the results of experiments and accompanying simulations are presented (Sect. 4).

2 Mixing on Rotating Platforms

The generic frame of reference for our centrifugal platform is the disk-based mixing module spinning at a frequency ν about an axis of rotation (Fig. 1). Neglecting gravity and capillarity, the only apparent force on a resting liquid plug of mass m placed in a radial channel at a mean radial position $\bar{r}$ is the centrifugal force

$$F_\nu = m\,\omega^2\,\bar{r} \tag{1}$$

with the angular frequency $\omega = 2\,\pi\,\nu$.

Assuming common no-slip boundary conditions on the channel walls ($\boldsymbol{u} = 0$), a parabolic radial velocity profile evolves with its maximum $u_{\max}$ located in the center of the channel. For a liquid with density ρ and viscosity η, a maximum velocity

$$u_{\max} = \frac{\rho\omega^2\bar{r}}{8\eta}\Delta x^2 \tag{2}$$

emerges in an idealized 2-dimensional fluidic channel (split stream) of width Δx and a mean radial position $\bar{r}$.

As soon as the liquid is in motion on the rotating disk, the Coriolis pseudo force

$$\boldsymbol{F}_{\mathrm{C}} = -2\,m\,\boldsymbol{\omega}\times\boldsymbol{u} \tag{3}$$

has to be taken into account scaling with the flow velocity $\boldsymbol{u}$.

$\boldsymbol{F}_{\mathrm{C}}$ is perpendicular to the axis of rotation and to the direction of flow, i.e., it points transversal to the direction of flow

[*] S. Haeberle (author to whom correspondence should be addressed, haeberle@imtek.de), T. Brenner, H.-P. Schlosser, R. Zengerle, J. Ducrée, IMTEK – University of Freiburg, Laboratory for MEMS Applications, Georges-Koehler-Allee 106, D-79110 Freiburg, Germany.

 DOI: 10.1002/ceat.200407138

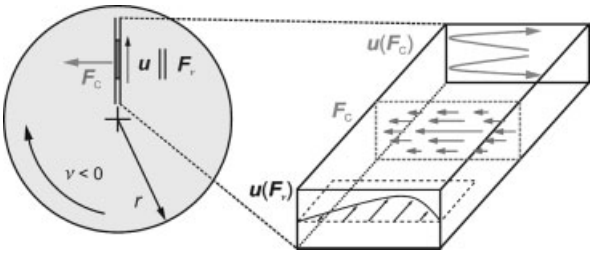

Figure 1. Two forces act on a flow as viewed in the rotating frame of reference, the centrifugal force $\boldsymbol{F}_\nu$ and the Coriolis pseudo force $\boldsymbol{F}_C$. The interplay of the inhomogeneous force field F_C with the confining side wall leads to a transverse "stirring" $\boldsymbol{u}(\boldsymbol{F}_C)$ within the mixing channel.

within the plane of the disk, and it peaks in the center of the channel at the maximum of the parabolic centrifugal flow profile.

The Coriolis force induces a transversal convection $\boldsymbol{u}(\boldsymbol{F}_C)$, which is confined by the side walls of the channel. Once arriving at the wall, the liquid must escape from the trailing liquid, which experiences a greater Coriolis force. It therefore travels backwards at the upper and lower part of the channel where it experiences the smallest Coriolis counter force.

This superposed perpendicular advective "stirring" adds to the radial movement of the liquid and thus increases the contact interface between the two liquid phases and enhances mixing. The effect is even more pronounced in low-(!) aspect-ratio channels since the enlargement of the contact interface scales with the width of the channel (see Fig. 4).

Beyond a certain threshold frequency

$$\nu_{th} = \frac{2\eta}{\pi\rho\,\Delta x^2} \tag{4}$$

the transverse Coriolis force even dominates the axial centrifugal force due to the different scaling of the forces $F_C \sim \nu^3$ and $F_\nu \sim \nu^2$ with the frequency of rotation ν. For a typical 200 μm width microchannel and water as a sample liquid, ν_{th} calculates to roughly 16 Hz.

Fig. 2 shows two color-tagged phases A and B merged at the beginning (①) of a channel in the simulation model (CFDRC-ACE+ [21]). After the fluid has passed a radial

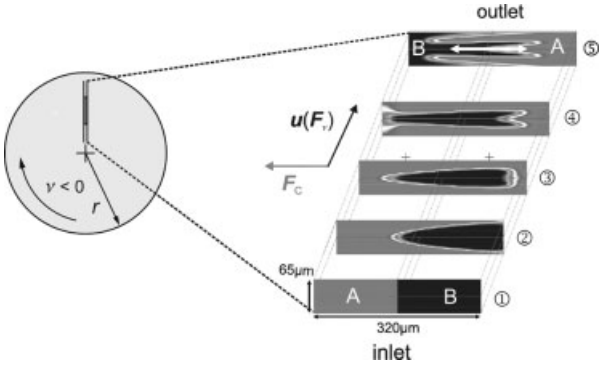

Figure 2. CFD simulation (CFDRC-ACE+ [21]) of a radial, low-aspect ratio mixing channel rotating at ν = –48 Hz.

channel length of 10 mm (③), the contact interface is increased by a factor of 9 (from 65 to ~600 μm) and continues to grow along the channel (phase-folding).

3 Setup and Flow Scheme

The microfluidic disk containing the mixing structures is mounted on a conventional drive unit, e.g., a standard lab centrifuge. Cylindrical reservoirs are placed concentrically on top of the mixing module for receiving the educts, which are dispensed by a (quasi-) continuous liquid jet during rotation (see Fig. 3). From there, the liquid educts are drawn by the centrifugal force into the microstructures. At the outer

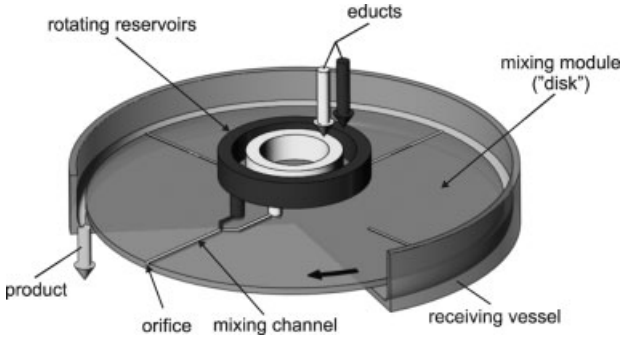

Figure 3. Schematic of the setup. The rotor unit ("disk") hosts the micromachined mixing structures. The liquid educts are continuously supplied by a free-jet dispenser to inlet reservoirs attached to the mixing module.

end of the mixing channel, the mixing product is centrifugally expelled from an orifice on the side surface of the module into the receiving vessel. The rotational symmetry of the mixing module strongly suggests a numbering up of mixing channels by a generic "wagon wheel" parallelization scheme.

The contact-free interfacing scheme obviates the need for pressure tight interconnects, thus shortening the down-time of the system and simplifying the maintenance of the modular setup of a reusable actuation unit and a possibly disposable mixing unit.

The simplest and intensively studied mixing structure comprises two different inlet channels, merged at a Y-conjunction into one common mixing channel (see Fig. 4) where the Coriolis-induced mixing process takes place. At the outer end of the channel, the mixing product is spun out of an orifice on the side surface of the module towards the wall of a receiving vessel (see Fig. 3). The asymmetry between the two inlet channels is described by a geometrical factor β. The centrifugal force $\boldsymbol{F}_\nu$ propels the radial flow through the channels while the transitional forces $\boldsymbol{F}_C$ and $\boldsymbol{F}_{clash}$ determine the position as well as the shape of the interfacial surface between the flows at the junction. This initial interface subsequently impacts the flow rate ratios and the downstream mixing process, which is governed by the Coriolis force and diffusion.

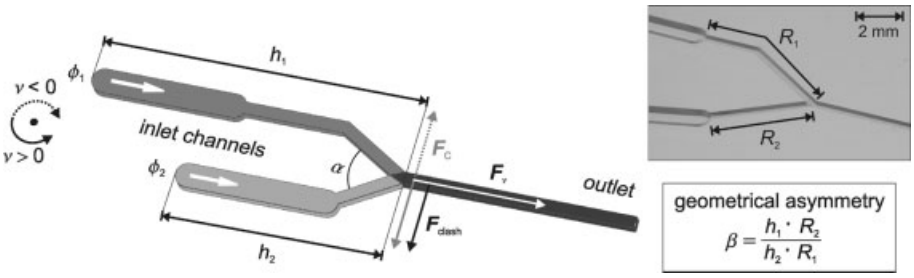

Figure 4. Layout of the Y-shaped mixing channel. Two separate inlet flows ϕ_1 and ϕ_2 are merged at an angle α and then driven through the radial mixing channel.

4 Experimental Results and Simulations

The micro reactor prototype has been experimentally qualified regarding volume throughput, mixing quality and flow rate ratios. Within the following sections, we present the main experimental results as well as the accompanying CFD-simulations (software package: CFDRC ACE+ V2004 [21]).

Throughput

As expected, the flow rates through rotating microchannels scale with the square of the spinning frequency ν (see Fig. 5). The composite outlet flow rate $\phi_1 + \phi_2$ only depends on ν, regardless of the sense of rotation. $\phi_1 + \phi_2$ is furthermore proportional to the inverse of the overall fluidic resistance R_{hd} of the mixing structure ($R_{hd,\beta\,=\,0.55} < R_{hd,\beta\,=\,1.5}$). Thus, the decrease of the flow rates towards elevated viscosities ($R_{hd} \sim \eta$) can, for instance, be compensated by increasing the frequency of rotation. Extrapolation of the experimental data towards higher frequencies results in an extraordinarily high volume throughput of 1 ml per second and channel at 90 Hz. All simulations and experiments were carried out using water as sample liquid.

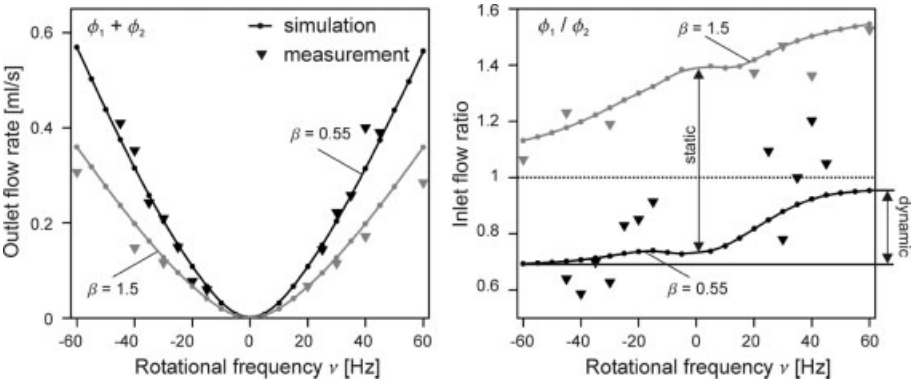

Figure 5. Left: The outlet flow rates through the radial mixing channel have been simulated and measured for two different asymmetric structures (β = 0.55 and β = 1.5). Right: The inlet flow ratio ϕ_1/ϕ_2 is statically set between 0.7 and 1.4 ($|\nu| < 60$ Hz) by the geometric coefficient β and can be adjusted online by the frequency ν. The experimental conditions become increasingly unstable and deviate from the simulations towards $\beta < 1$.

Mixing Performance

Apart from the volume throughput, the most important characteristics of a mixer are the homogeneity of the product. The mixing performance of the centrifugal micromixer has been determined using the formerly introduced competitive Villermaux reaction scheme [22]. This reaction allows the calculation of the micromixedness ratio γ representing the quality of mixing ($\gamma = 0$ equals "no" mixing). The measured micromixedness ratios for the centrifugal Coriolis mixer range from 14 at a volume throughput of 0.1 mL s^{-1} to 807 at 0.97 mL s^{-1}. Compared to approximated values (interdigital mixer: 2313 at 0.13 mL s^{-1}, caterpillar mixer: 148 at 0.67 mL s^{-1} [23]) of other micromixers, a previously unexplored region of high mixing quality at high volume throughput ("powermixing") is reached (see Fig. 6).

Process Control

Active control of flow rates and flow ratios is of paramount interest in continuous flow microreactors. In our novel centrifugal mixing scheme, the flow ratio in the mixing channel (see Fig. 4) is statically defined by the asymmetry and the hydrodynamic resistances of the two inlet channels which are incorporated into the geometric coefficient β.

Furthermore, the flow rate ratio can be adjusted dynamically via the frequency of rotation ν, utilizing different scaling of the impact forces with ν. Namely, these are the centrifugal force $\boldsymbol{F}_\nu \sim \nu^2$ governing the radial flow components and the resulting transversal force $\boldsymbol{F}_{clash} + \boldsymbol{F}_C$ defining the position of the interfacial surface between the incoming flows at their first contact within the junction. The first constituent, the "clash force" $\boldsymbol{F}_{clash}$, accounts for the deviating pressure heads across the inlet channels and the difference in the kinetic energies, i.e., the inertia of the so-induced substreams ϕ_1 and ϕ_2. The other impact force is the Coriolis pseudo force $\boldsymbol{F}_C \sim \nu^3$ whose direction is selected by the sign of ν. Towards elevated ν, $\boldsymbol{F}_C$ acts as a frequency-adjustable setscrew to shape the contact surface within the junction. Fig. 7 shows the dynamic control of flow ratio from 1.22 to 1.38 between frequencies of –35 Hz and –5 Hz, respectively.

Reversing the sense of rotation ($\nu > 0$), $\boldsymbol{F}_C$ now supports $\boldsymbol{F}_{clash}$ to

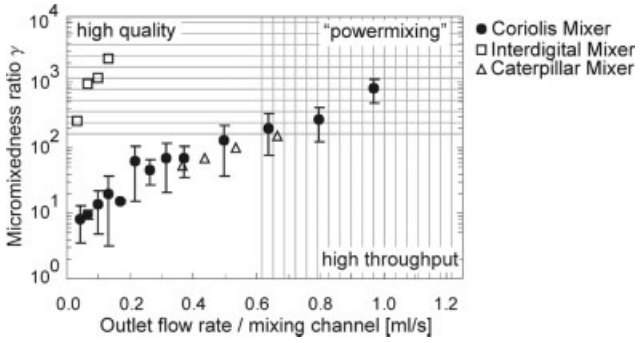

Figure 6. Micromixedness ratio as a function of the outlet flow rate ($\phi_1 + \phi_2$) through a single mixing channel. The quality of mixing increases up to 801 towards very high volume throughputs (0.97 ml / s). Literature values of other micromixers are given to range the experimentally acquired data [23].

suppress ϕ_2. Beyond a critical frequency, a new type of lateral advection is observed within the junction (see Fig. 7, 35 Hz). It is attributed to the hydrodynamic "thumb" pushed by $\boldsymbol{F}_{\text{clash}} + \boldsymbol{F}_{\text{C}}$ against the flow ϕ_2. As the parabolic velocity profile peaks in the center, ϕ_2 is forced to escape in a tight jet along the perimeter of the "thumb" where the velocity dependent counterforce $\boldsymbol{F}_{\text{C}}$ is minimum. This jet injection provides a means to actively accelerate mixing prior to the previously described Coriolis induced advective mixing along the channel.

5 Conclusions

We introduced a novel centrifugal microreaction platform based on the Coriolis induced mixing within simple microfluidic channels. The Coriolis micromixer excels with fast mixing at extraordinarily high volume throughputs. Thus, a major bottleneck of micromixing technology could be appreciably widened. Also the possibility to actively control flow rates and flow ratios by changing the sense and frequency of rotation has been demonstrated.

The modular setup comprising reusable "macro" components and a readily exchangeable, possibly disposable disk also significantly simplifies maintenance, reduces down times and eventually saves costs.

Acknowledgements

The authors are grateful to the support by the "Landesstiftung Baden-Württemberg gGmbH" and enjoyed an excellent cooperation with HSG-IMIT and the group of Willi Bannwarth at the University of Freiburg.

Received: December 10, 2004 [CET 7138]

References

[1] W. Ehrfeld, H. Löwe, V. Hessel, T. Richter, *Chem. Ing. Tech.* **1996**, *68* (*9*), 1091.
[2] H. Löwe, W. Ehrfeld, *Electrochim. Acta* **1999**, *44* (*21–22*), 3679.
[3] V. Hessel, S. Hardt, H. Löwe, *Chemical Micro Process Engineering – Fundamentals, Modelling and Reactions*, Wiley-VCH, Weinheim **2004**.
[4] H. Pennemann et al., *Org. Process Res. Dev.* **2004**, *8*, 422.
[5] G. M. Greenway et al., *Sens. Actuators, B* **2000**, *63* (*3*), 153.
[6] K. F. Jensen, *Chem. Eng. Sci.* **2001**, *56*, 293.
[7] J. Melin et al., *Lab on a Chip* **2004**, *4*, 214.
[8] W. Ehrfeld et al., *Ind. Eng. Chem. Res.* **1999**, *38* (*3*), 1075.
[9] F. G. Bessoth, A. J. deMello, A. Manz, *Anal. Commun.* **1999**, *36* (*6*), 213.
[10] M. Koch, C. G. J. Schabmueller, A. G. R. Evans, A. Brunnschweiler, *Sens. Actuators, A* **1999**, *74*, 207.
[11] M. Heule, A. Manz, *Lab on a Chip* **2004**, *4*, 506.
[12] D. Bökenkamp et al., *Anal. Chem.* **1998**, *70*, 232.
[13] J. Lichtenberg, H. Baltes, in *Proc. of μTAS 2004* (Eds: T. Laurell, J. Nilsson, K. Jensen, D. J. Harrison, J. P. Kutter), The Royal Society of Chemistry, Cambridge **2004**, 351.
[14] C. A. Burtis et al., *Clin. Chem.* **1972**, *18* (*8*), 753.
[15] C. T. Schembri et al., *J. Autom. Chem.* **1995**, *17* (*3*), 99.
[16] M. Madou, G. Kellogg, in *Proc. of SPIE, Vol. 3259* (Eds: G. E. Cohn), The International Society for Optical Engineering, Bellingham **1998**, 80.
[17] M. Madou, Y. Lu, S. Lai, J. Lee, S. Daunert, in *Proc. of the μTAS 2000* (Eds: A. van den Berg, P. Bergveld), Kluwer Academic Publisher, Dordrecht **2000**, 565.
[18] G. Ekstrand et al., in *Proc. of the μTAS 2000* (Eds: A. van den Berg, P. Bergveld), Kluwer Academic Publisher, Dordrecht **2000**, 311.
[19] J. Ducrée, T. Brenner, T. Glatzel, R. Zengerle, in *Proc. of μTAS 2003* (Eds: M. A. Northrup, K. F. Jensen, D. J. Harrison), Transducers Research Foundation, San Diego **2003**, 603.
[20] J. Ducrée, H-P. Schlosser, T. Glatzel, S. Haeberle, M. Grumann, T. Brenner, R. Zengerle, in *Proc. of μTAS 2004* (Eds: T. Laurell, J. Nilsson, K. Jensen, D. J. Harrison, J. P. Kutter), The Royal Society of Chemistry, Cambridge **2004**, 554.
[21] CFD Research Corporation, http://www.cfdrc.com (accessed Dec. **2004**).
[22] M.-C. Fournier, L. Falk, J. Villermaux, *Chem. Eng. Sci.* **1996**, *51*, 5053.
[23] S. Panic, S. Loebbecke, T. Tuercke, J. Antes, D. Boškovic, *Chem. Eng. J.* **2004**, *101*, 409.

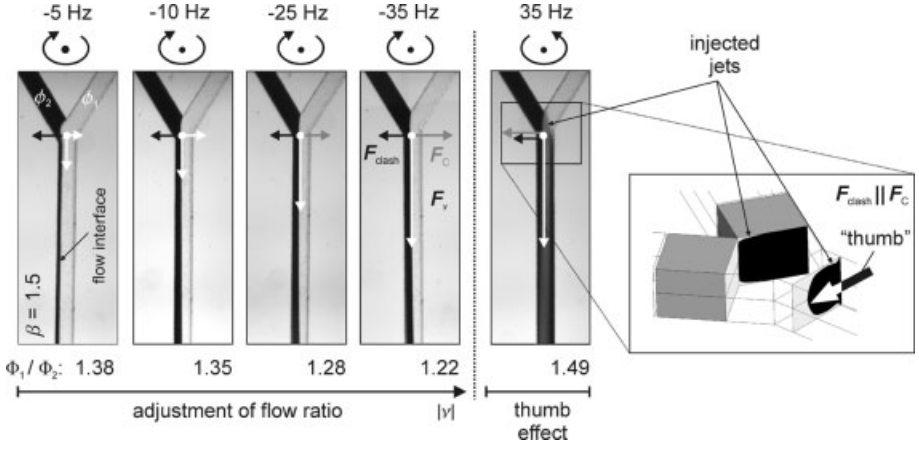

Figure 7. Pure water and aqueous ink are chosen to investigate the hydrodynamic effects within the junction of the two inlets. The static ratio of approximately 1.4 originates from the asymmetry of the structure ($\beta = 1.5$). Changing the sense of rotation leads to an additional mixing ("thumb effect") at the junction.

